Video Article

Calcification of Vascular Smooth Muscle Cells and Imaging of Aortic Calcification and Inflammation

Caitlin O'Rourke*[1], Georgia Shelton*[1,2], Joshua D. Hutcheson[3,4], Megan F. Burke[2], Trejeeve Martyn[1], Timothy E. Thayer[2], Hannah R. Shakartzi[1], Mary D. Buswell[1], Robert E. Tainsh[1], Binglan Yu[1,4], Aranya Bagchi[1,4], David K. Rhee[2,4], Connie Wu[1,2,4], Matthias Derwall[5], Emmanuel S. Buys[1,4], Paul B. Yu[3,4], Kenneth D. Bloch[1,2,4], Elena Aikawa[3,4], Donald B. Bloch[1,5,6], Rajeev Malhotra[2,4]

[1]Anesthesia Center for Critical Care Research of the Department of Anesthesia, Critical Care, and Pain Medicine, Massachusetts General Hospital

[2]Cardiovascular Research Center and Cardiology Division of the Department of Medicine, Massachusetts General Hospital

[3]Cardiovascular Division, Brigham and Women's Hospital

[4]Harvard Medical School

[5]Department of Anesthesiology, Uniklinik RWTH Aachen, RWTH Aachen University

[6]Center for Immunology and Inflammatory Diseases and the Division of Rheumatology, Allergy, and Immunology of the Department of Medicine, Massachusetts General Hospital

*These authors contributed equally

Correspondence to: Rajeev Malhotra at rmalhotra@mgh.harvard.edu

URL: https://www.jove.com/video/54017
DOI: doi:10.3791/54017

Keywords: Medicine, Issue 111, vascular calcification, smooth muscle cell, matrix gla protein, atherosclerosis, macrophage, near-infrared fluorescent imaging, vascular inflammation

Date Published: 5/31/2016

Citation: O'Rourke, C., Shelton, G., Hutcheson, J.D., Burke, M.F., Martyn, T., Thayer, T.E., Shakartzi, H.R., Buswell, M.D., Tainsh, R.E., Yu, B., Bagchi, A., Rhee, D.K., Wu, C., Derwall, M., Buys, E.S., Yu, P.B., Bloch, K.D., Aikawa, E., Bloch, D.B., Malhotra, R. Calcification of Vascular Smooth Muscle Cells and Imaging of Aortic Calcification and Inflammation. *J. Vis. Exp.* (111), e54017, doi:10.3791/54017 (2016).

Abstract

Cardiovascular disease is the leading cause of morbidity and mortality in the world. Atherosclerotic plaques, consisting of lipid-laden macrophages and calcification, develop in the coronary arteries, aortic valve, aorta, and peripheral conduit arteries and are the hallmark of cardiovascular disease. In humans, imaging with computed tomography allows for the quantification of vascular calcification; the presence of vascular calcification is a strong predictor of future cardiovascular events. Development of novel therapies in cardiovascular disease relies critically on improving our understanding of the underlying molecular mechanisms of atherosclerosis. Advancing our knowledge of atherosclerotic mechanisms relies on murine and cell-based models. Here, a method for imaging aortic calcification and macrophage infiltration using two spectrally distinct near-infrared fluorescent imaging probes is detailed. Near-infrared fluorescent imaging allows for the *ex vivo* quantification of calcification and macrophage accumulation in the entire aorta and can be used to further our understanding of the mechanistic relationship between inflammation and calcification in atherosclerosis. Additionally, a method for isolating and culturing animal aortic vascular smooth muscle cells and a protocol for inducing calcification in cultured smooth muscle cells from either murine aortas or from human coronary arteries is described. This *in vitro* method of modeling vascular calcification can be used to identify and characterize the signaling pathways likely important for the development of vascular disease, in the hopes of discovering novel targets for therapy.

Video Link

The video component of this article can be found at https://www.jove.com/video/54017/

Introduction

Cardiovascular disease is the leading cause of morbidity and mortality in the world, including the United States where it accounts for over 780,000 deaths annually.[1] Coronary artery calcification and aortic calcification are hallmarks of atherosclerotic disease and serve as strong predictors of cardiovascular events.[2-4] Two main types of vascular calcification have been reported in adults: intimal calcification, associated with atherosclerosis, and medial (also known as Mönckeberg) calcification, associated with chronic kidney disease and diabetes.[5] Intimal calcification occurs in the setting of lipid accumulation and macrophage infiltration into the vessel wall.[5,6] Medial wall calcification occurs independently of intimal calcification, localizes to elastin fibers or smooth muscle cells, and is not associated with lipid deposition or macrophage infiltration.[5,7,8] Studies on the molecular mechanisms of vascular calcification have relied on cell-based and animal model systems. Rodent models for atherocalcific disease include mice deficient in either apolipoprotein E (ApoE)[9,10] or low-density lipoprotein receptor (LDLR)[11] fed a high-fat diet, while models for medial calcification include mice with matrix Gla protein (MGP) deficiency[12] or rats that develop uremia either by near total nephrectomy (the 5/6th nephrectomy model) or by exposure to a high-adenine diet.[13]

Here, the model of medial vascular calcification associated with MGP deficiency is focused on. MGP is an extracellular protein that inhibits arterial calcification.[12] Mutations in the *MGP* gene have been identified in Keutel syndrome, a rare human disease characterized by diffuse cartilage calcification in addition to brachytelephalangy, hearing loss, and peripheral pulmonary stenosis.[14-18] Although not often observed,[19]

concentric calcification of multiple arteries has been described in Keutel syndrome.[20] Common polymorphisms in the human *MGP* gene are associated with increased risk for coronary artery calcification,[21-23] while higher circulating levels of uncarboxylated, biologically inactive MGP predict cardiovascular mortality.[24] Unlike humans with Keutel syndrome, MGP-deficient mice develop a severe vascular phenotype consisting of spontaneous widespread arterial calcification starting at two weeks of age and die 6-8 weeks after birth due to aortic rupture.[12]

Unlike ApoE$^{-/-}$ and LDLR$^{-/-}$ mice fed a high-fat diet, which develop intimal vascular calcification with associated macrophage-induced inflammation, MGP$^{-/-}$ mice develop medial vascular calcification in the absence of macrophage infiltration.[11,25] Although these findings suggest different underlying stimuli for intimal and medial calcification, there is overlap in the signaling mechanisms that mediate both forms of calcification.[26] Multiple signaling pathways have been identified that contribute to vascular calcification including inflammatory mediators such as tumor necrosis factor-α and IL-1 and pro-osteogenic factors such as Notch, Wnt, and bone morphogenetic protein (BMP) signaling.[27,28] These signaling pathways increase expression of the transcription factors runt-related transcription factor 2 (Runx2) and osterix, which in turn increase expression of bone-related proteins (*e.g.*, osteocalcin, sclerostin, and alkaline phosphatase) in the vasculature that mediate calcification.[28-30] We and others have demonstrated that the vascular calcification observed in ApoE$^{-/-}$ and LDLR$^{-/-}$ mice fed a high-fat diet and the spontaneous vascular calcification observed in MGP$^{-/-}$ mice all depend on bone morphogenetic protein (BMP) signaling, and it is this pathway that is focused on here.[11,25,31] BMPs are potent osteogenic factors required for bone formation and are known to exhibit increased expression in human atherosclerosis.[32-34] *In vitro* studies have implicated BMP signaling in regulating the expression of osteogenic factors such as Runx2.[35-37] Overexpression of the BMP ligand, BMP-2, accelerates the development of vascular calcification in ApoE-deficient mice fed a high fat diet.[38] Moreover, the use of specific BMP signaling inhibitors such as LDN-193189 (LDN)[39,40] and/or ALK3-Fc prevents the development of vascular calcification in both LDLR$^{-/-}$ mice fed a high-fat diet and MGP-deficient mice.[11,25]

Vascular smooth muscle cells (VSMCs) have a critical role in the development of vascular calcification.[30,41,42] The medial vascular calcification that develops in MGP-deficient mice is characterized by a transdifferentiation of VSMCs to an osteogenic phenotype. Loss of MGP results in decreased expression of VSMC markers including myocardin and alpha smooth muscle actin, with a concomitant rise in osteogenic markers such as Runx2 and osteopontin. These changes coincide with the development of vascular calcification.[25,43,44]

Aortic calcification and inflammation in mice are typically assessed utilizing histochemical techniques such as alkaline phosphatase activity for early calcification and osteogenic activity, von Kossa and Alizarin red staining for late calcification, and immunohistochemical protocols that target macrophage protein markers (*e.g.*, CD68, F4/80, Mac-1, Mac-2, Mac-3).[9,45] However, these standard imaging techniques require processing of aortic tissues into cross-sections, which is time consuming and imperfect due to sampling bias, and are limited in their ability to quantify inflammation and calcification in the whole aorta. This protocol describes a method to visualize and quantify whole aortic and medium-sized arterial calcification and macrophage accumulation utilizing near-infrared fluorescent (NIR) molecular imaging *ex vivo.* Also provided is a method for harvesting and culturing primary aortic VSMCs from mice and inducing the calcification of murine and human VSMCs *in vitro* in order to determine the molecular mechanisms underlying vascular calcification. These techniques provide the investigator with both *in vivo* and *in vitro* methods for studying atherocalcific disease.

Protocol

All studies with mice were performed in strict accordance with the recommendations in the Guide for the Care and Use of Laboratory Animals of the National Institutes of Health. Housing and all procedures involving mice described in this study were approved by the Institutional Animal Care and Use Committees of Massachusetts General Hospital (Subcommittee on Research Animal Care). All procedures were performed with care to minimize suffering.

1. Preparation of Reagents

1. Near-Infrared Fluorescence Imaging of Whole Aortas
   Note: A bisphosphonate-derived, near-infrared fluorescent imaging probe can be used to mark osteogenic activity in the vasculature by binding to hydroxyapatite.[46,47] A cathepsin-activated fluorescent imaging probe can serve as a marker for macrophage proteolytic and elastolytic activity in the vasculature.[9] To permit the simultaneous use of both fluorescent probes, it is important to use probes that are spectrally distinct. The notation calcium NIR will be used to indicate the calcification-specific near-infrared fluorescent imaging probe and cathepsin NIR to indicate the cathepsin activity-specific near-infrared fluorescent imaging probe.
   1. Prepare the solutions of calcium NIR and cathepsin NIR. As per manufacturer's protocols, add 1.2 ml of 1x phosphate buffered saline (PBS) to the vial containing 24 nmol of calcium NIR or cathepsin NIR and shake gently.
      Note: According to the manufacturer, once reconstituted with PBS, the calcium NIR and cathepsin NIR solutions remain stable for 14 days when stored in the dark at 2-8 °C.

2. Isolation and Calcification of Murine Aortic VSMCs
   1. Aortic Digestion Solution:
      1. Prepare a fresh solution (~3-5 ml per aorta harvested) with Hank's Balanced Salt Solution (HBSS) containing 175 U/ml type 2 collagenase and 1.25 U/ml elastase. Sterilize the solution with a 0.22 µm vacuum-driven filtration system and keep the solution on ice until use.

   2. Cell Media:
      1. Supplement 500 ml of Dulbecco's Modified Eagle Medium (DMEM) with 10% fetal bovine serum, 100 units/ml penicillin, and 100 µg/ml streptomycin. Warm the media to 37 °C prior to use.

   3. Calcification Media:
      1. Calcification Media A (NaPhos; used in mouse cell lines):
         1. Supplement 100-500 ml of DMEM (volume as needed) with 10% fetal bovine serum, 2 mM sodium phosphate, 100 units/ml penicillin, and 100 µg/ml streptomycin. Warm the media to 37 °C prior to use.

OR

2. Calcification Media B (βGP/Asc/DEX; used in either mouse or human cell lines):
    1. Supplement 100-500 ml of DMEM (volume as needed) with 10% fetal bovine serum, 10 mM β-glycerophosphate disodium, 50 µg/ml L-ascorbic acid, 10 nM dexamethasone, 100 units/ml penicillin, and 100 µg/ml streptomycin. Warm the media to 37 °C prior to use.

2. Tail Vein Injection

1. Before tail injection, warm the mice under a mild heating lamp for 5 min.
2. Restrain the mouse in a tube rodent holder. Disinfect the tail with an alcohol swab.
3. Utilize a 30 G needle for tail vein injection. Tail veins are located laterally.
    1. Apply a gentle amount of forward pressure on the syringe as the needle is advanced into the tail. The vein is accessed once the resistance to injection is no longer present.
    2. Inject a volume of 100 µl of calcium NIR and/or 100 µl of cathepsin NIR at a steady rate. At the end of injection, after a 5 sec pause, withdraw the needle.
4. Harvest the aortas (see section 3) 3-24 hr after injection.

3. Mouse Dissection

1. Euthanize mouse with a 200 mg/kg intraperitoneal pentobarbital injection.
2. Lay the animal supine on the dissection board and stabilize by taping each paw to the board. Using a dissecting microscope and small scissors, make a midline incision extending from the lower abdomen to the upper thorax.
3. Peel back the skin with forceps and remove the peritoneum, revealing the abdominal organs. Remove the gastrointestinal organs, taking care not to transect the aorta.
4. Make a lateral incision in the anterior diaphragm and continue the incision across the abdomen. Using dissection scissors, release the ribcage by cutting through the sides of the ribs and removing the soft tissue adherent to the superior portion of the sternum. Remove the ribcage, revealing the lungs.
5. Leave the heart in place initially (to aid in identifying and dissecting the proximal aorta) and carefully remove the lungs. Remove the thymus, trachea, and esophagus with care, ensuring that the aorta remains intact.
6. Using straight fine forceps and micro-dissecting scissors, remove the soft tissue surrounding the aorta from the iliac bifurcation to the aortic arch, paying careful attention when removing the peri-aortic fat (**Figure 1A**). Remove the remaining fat and soft tissue surrounding the large branches of the aortic arch (*i.e.*, brachiocephalic, common carotid and subclavian arteries, **Figure 1B**).
   Note: It is important to remove the fat from the aorta because fat can increase the background signal when performing fluorescence imaging.
7. Remove the heart from the thoracic cavity, carefully detaching it from the proximal aorta, and discard. Transect the distal aorta at the iliac bifurcation. Using an insulin needle, inject normal saline into the aorta from the aortic arch to wash out remaining blood cells. Detach the aorta along with the aortic arch vessels, completely removing it from the body.
8. Place the aorta in normal saline solution on ice until ready for imaging.

4. Aortic Imaging

1. Image aortas *ex vivo* immediately after harvest by near-infrared fluorescence reflectance imaging.[25]
    1. Set the fluorescence imager at the appropriate multichannel wavelengths to quantify fluorescence signal intensities from the aortas of calcium NIR and cathepsin NIR-injected mice, as previously described.[25] According to the manufacturer, calcium NIR can be excited by ~ 650-678 nm light with a maximal emission in the ~ 680-700 nm range. Cathepsin NIR can be excited by ~ 745-750 nm light with a maximal emission at ~770 nm.

5. Isolation of Primary Murine Aortic Vascular Smooth Muscle Cells

1. Perform steps 3.1-3.7 as described above.
2. Place aortas in cold HBSS until the dissections are complete. Carefully cut away any remaining periaortic fat and soft tissue, leaving only the aorta.
3. Under a sterile tissue culture hood, transfer the aortas to the Aortic Digestion Solution in 35 mm x 10 mm tissue culture dishes. Place in an incubator at 37 °C for 30 min with gentle intermittent rocking. After digestion, the aortas exhibit a stretched or frayed appearance.
4. With the dissection microscope and sterile forceps, remove the outer adventitial layer of the aorta while keeping the medial layer intact. One technique for removing the adventitia is to peel away the outer layer of the aorta at one end and remove it from the underlying medial layer like a sock could be peeled back and removed.
5. Once the adventitial layer has been removed, place the remaining aorta into a new tissue culture dish with cell culture media and store at 37 °C with 5% CO_2 for 2-4 hr.
6. Under a sterile hood and using sterile 3 mm micro-dissection scissors, cut the aorta into 1-2 mm wide rings.
7. Place these rings in a new tissue culture dish with Aortic Digestion Solution and incubate at 37 °C with gentle intermittent rocking for 120 min. Pipette the solution up and down several times during this incubation to resuspend cells.

8. Add 5 ml of warm cell culture media to the digestion solution and transfer to a 15 ml conical tube.
9. Centrifuge the tube for 5 min at 200 x g.
10. Aspirate the media and resuspend cells in the desired volume of cell culture media (*e.g.*, 5 ml).
11. Plate the entire amount of isolated cells from each aorta in a 25 cm^2 cell culture flask and incubate at 37 °C with 5% CO_2. Propagate cells using standard techniques, as previously described.[25,48] During the initial 7-10 days of incubation, change the media every 72-96 hr. As the cells approach confluence, replenish media more frequently (every 48 hr).
    Note: It may take many weeks to grow a sufficient quantity of cells.
12. Once confluent, passage cells with trypsin that is warmed to 37 °C.
    1. Add 0.5-1.0 ml of trypsin to each culture flask and incubate for 3-5 min; gently tap the side of the flask every 30-60 sec as needed to detach cells from the surface.
    2. Once the cells detach from the bottom of the flask, add 10 ml of cell media to the cells in trypsin. Centrifuge the cells at 200 x g for 5 min. Aspirate the media and trypsin from the cell pellet. Resuspend the cells in the desired amount of fresh cell media (*e.g.*, 5-10 ml) and transfer to a new flask (with some cells transferred to a chamber slide).
13. At the first passage of cells, confirm the smooth muscle cell lineage with standard immunocytochemistry techniques, as previously described,[49] using an antibody directed against α-smooth muscle actin.

6. Inducing Calcification of Cultured Smooth Muscle Cells

1. Plate cells obtained from 5.12 in a 6-well format. Note: Starting with 1 x 10^5 cells/well in a total volume of 2.0 ml of cell media per well is recommended.
2. Allow cells to grow in Calcification Media A or B for at least 7 days in a 6-well plate format. Incubate cells at 37 °C with 5% CO_2.
3. Change cell media every 48 hr.

7. Assessing VSMC Calcification Using the von Kossa Staining Method

Note: The von Kossa method for measuring extracellular matrix calcification of tissues or cultured cells is based on the substitution of phosphate-bound calcium ions with silver ions.[50] In the presence of light and organic compounds, the silver ions are reduced and visualized as metallic silver. Any unreacted silver is removed by treatment with sodium thiosulfate.[50] The protocol for von Kossa staining is as follows:

1. Aspirate media from cell culture plates.
2. Fix cells by placing them in 1 ml of 10% formalin at room temperature for 20 min.
3. Remove the formalin and wash the fixed cells with distilled water for 5 min.
4. Incubate cells in 1 ml of 5% silver nitrate solution under a 60-100 W bulb for 1-2 hr.
5. Aspirate the silver nitrate solution and wash with distilled water for 5 min.
6. Remove unreacted silver by placing the cells in 1 ml of 5% sodium thiosulfate (w/v) solution in distilled water for 5 min.
7. Rinse cells with distilled water for 5 min. Repeat washes 3x. The von Kossa stain is ready for imaging with standard inverted light microscopy.
8. Optional Step: Counterstain with 1ml of nuclear fast red for 5 min. Follow this with three washes with distilled water (5 min each).

OR

8. Assessing VSMC Calcification with Near-infrared Fluorescent Imaging

Note: Similar to its ability to identify calcification within mouse aortas, calcium NIR readily binds calcific mineral deposited by cultured cells. Using this technique, fluorescent microscopy and plate readers with long wavelength filters can image and quantify *in vitro* calcification, respectively. The long wavelength emission of the calcium NIR allows for the simultaneous utilization of lower wavelength emitting fluorophores to detect other features. The protocol for calcium NIR staining is as follows:

1. As described in Section 1.1.1, add 1.2 ml of 1x PBS to the vial containing 24 nmol of calcium NIR.
2. Dilute the calcium NIR stock 1:100 in the appropriate calcification or control media.
3. Aspirate cell media from culture plates and replace with the calcium NIR-containing culture media.
4. Incubate the culture plates with calcium NIR media overnight at 37 °C.
5. Aspirate the media from the wells and wash the wells once with PBS.
    Note: At this point, the original culture media can be added to the wells, and the cells can be imaged live. Otherwise, proceed to the steps below.
6. Fix cells by placing them in 1 ml of 10% formalin at room temperature for 20 min.
7. Remove the formalin and wash the fixed cells with distilled water for 5 min. Repeat washes 3x.
8. Optional step: Perform immunofluorescence staining or other counterstains for proteins of interest.[8,9]
9. Image or detect the calcium NIR stain using appropriate fluorescence excitation wavelengths (*e.g.*, calcium NIR can be excited by 650-678 nm light) and emission filters (~ 680-700 nm).

Representative Results

Aortic calcification in MGP$^{-/-}$ and wild-type mice was measured using imaging of calcium NIR fluorescence. No calcium NIR signal was detected in the aortas from wild-type mice, indicating the absence of calcification (**Figure 2**). A strong calcium NIR signal was detected in the aortas from MGP-deficient mice, which is consistent with advanced vascular calcification. Tissue sections of aortas from wild-type and MGP$^{-/-}$ mice were stained with Alizarin red[25] (**Figure 3A**-**B**), confirming the extensive vascular calcification observed in MGP-deficient mice with no calcification detected in wild-type mice. To determine whether the vascular calcification associated with MGP deficiency is dependent on BMP signaling, MGP$^{-/-}$ mice were treated with LDN, ALK3-Fc, or vehicle starting at day 1 of life. These mice were injected with calcium NIR on day 27 and aortas were harvested the following day. Pharmacologic inhibition of BMP signaling reduced aortic calcification detected with calcium NIR (**Figure 2**). Similar to the findings with calcium NIR, the aortas of LDN- and ALK3-Fc-treated MGP$^{-/-}$ mice had reduced Alizarin red stain for calcium when compared to vehicle-treated MGP$^{-/-}$ mice (**Figure 3B**-**D**). These results indicate that BMP signaling is required for the vascular calcification observed in MGP$^{-/-}$ mice.

LDLR$^{-/-}$ mice fed a high fat diet develop both macrophage inflammation and calcification of the arterial wall.[11] Simultaneous tail vein injection of calcific and cathepsin-specific NIR probes in MGP$^{-/-}$ mice was performed to determine if the vascular calcification of MGP-deficiency is associated with macrophage accumulation.[25] LDLR$^{-/-}$ mice fed a high fat diet and wild-type mice were used as positive and negative controls, respectively. Aortas from wild-type mice exhibited virtually no calcium NIR or cathepsin NIR signal, as anticipated (**Figure 4A**). Co-localized calcium NIR and cathepsin NIR signals that favored the aortic arch region were observed in the LDLR$^{-/-}$ mice, indicating a strong association between macrophage infiltration and vascular calcification in this model of intimal atherosclerosis. Although a diffuse and strong calcium NIR signal was observed in the aortas of MGP$^{-/-}$ mice, the cathepsin NIR signal was no different from that of wild-type mice. These findings indicate that the vascular calcification in MGP deficiency occurs in the absence of macrophage accumulation. To further confirm these findings, aortas from wild-type, MGP$^{-/-}$, and LDLR$^{-/-}$ mice were harvested, sectioned, and stained with an antibody specific for the macrophage marker MAC-2 (**Figure 4B**). The aortas from LDLR$^{-/-}$ mice demonstrated abundant MAC-2 staining; there was no detectable MAC-2 staining in the aortas of MGP$^{-/-}$ mice, indicating an absence of vascular macrophages.

To model vascular calcification *in vitro*, aortic VSMCs were isolated from wild-type and MGP$^{-/-}$ mice and cultured in high-phosphate containing media, using the protocol described above. To determine the role of MGP in modulating calcification of cultured VSMCs, an adenovirus expressing MGP (Ad.MGP) was used to restore MGP in aortic VSMCs from MGP$^{-/-}$ mice. MGP-deficient VSMCs infected with an adenovirus expressing green fluorescent protein (Ad.GFP) were used as control. In addition, to determine the effect of removing MGP expression from VSMCs on subsequent calcification, aortic VSMCs from wild-type mice were treated with siRNA directed against MGP (siMGP) or control siRNA (siSC). Calcification was induced in cultured VSMCs by growing the cells in Calcification Media A for 7 days. Cells were subsequently fixed and stained for calcium using the von Kossa method. Restoration of MGP with Ad.MGP reduced calcification of MGP$^{-/-}$ VSMCs compared to control adenovirus-treated cells (**Figure 5A**-**B**, **E**). Treatment of wild-type aortic VSMCs with siMGP, resulting in >95% knockdown of MGP expression,[25] increased calcification compared to siSC-treated cells (**Figure 5C**-**D**, **F**). These results indicate that this *in vitro* model of VSMC calcification mimics the findings in MGP-deficient mice and demonstrates that MGP modulates calcification of cultured VSMCs.

An alternative method to detecting calcification of cultured VSMCs is with calcium NIR. To model vascular calcification *in vitro*, human coronary artery VSMCs were purchased and cultured for 21 days in Calcification Media B. Following the treatment period, calcification was identified using the calcium NIR method and the cultures were counterstained with a custom green-fluorescent collagen probe[51] and Hoechst dye (1 µg/ml for 5 min after fixation in 10% formalin) (**Figure 6**). VSMC nuclei were observed with blue Hoechst fluorescence by confocal microscopy (**Figure 6A**). A representative optical section shows calcium NIR-stained calcific mineral within the collagen matrix produced by the VSMCs (**Figure 6B**). Three-dimensional reconstructions of optical z-stacks illustrate the layers created in culture as the VSMCs on the bottom of the well produce a collagen matrix in which the deposited calcific mineral becomes entrapped (**Figure 6C**-**D**).

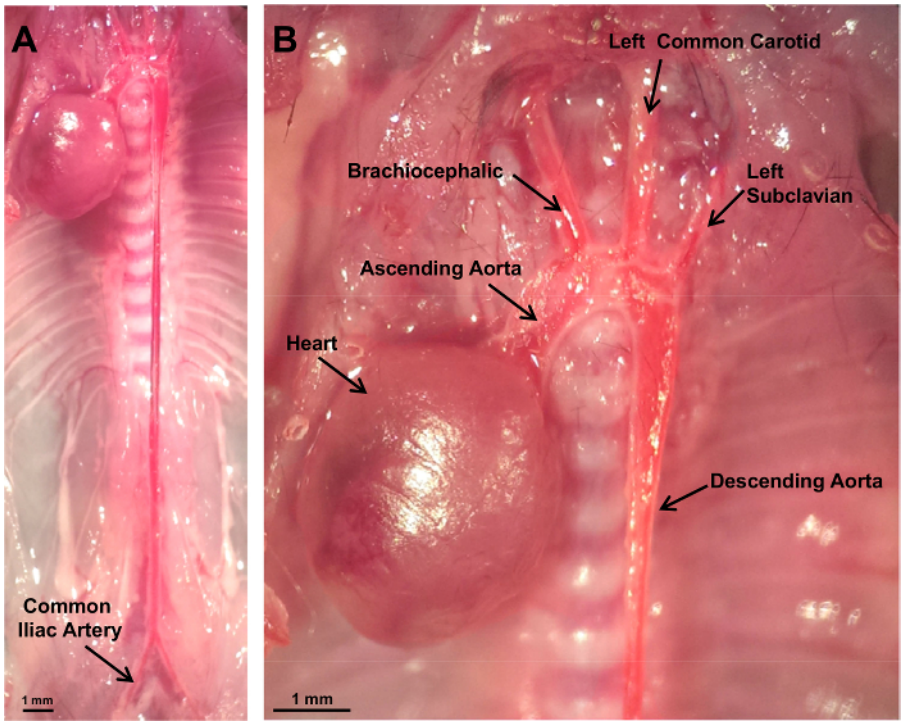

Figure 1: Representative Dissection of an Aorta from a Wild-type Mouse. (**A**) A picture of the thoracic and abdominal aorta extending to the common iliac artery bifurcation is depicted after removal of the overlying organs and peri-aortic fat. (**B**) A focused view of the aortic arch with the brachiocephalic, left common carotid, and left subclavian arteries. Scale bars = 1 mm. Please click here to view a larger version of this figure.

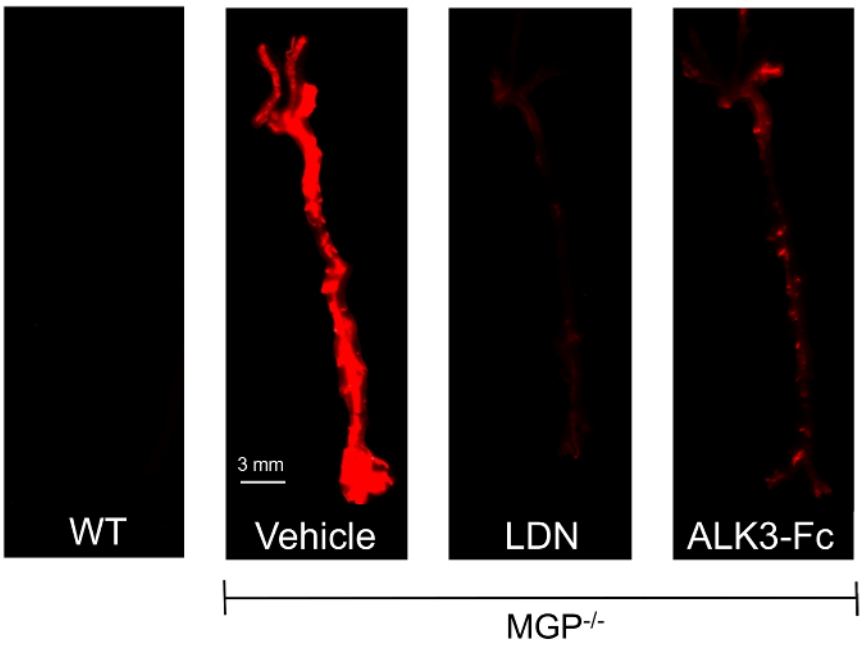

Figure 2: Vascular Calcification in MGP$^{-/-}$ mice is Dependent on BMP Signaling. MGP$^{-/-}$ mice were treated with intraperitoneal (i.p.) injections of either vehicle, LDN-193189 (LDN, 2.5 mg/kg/day), or ALK3-Fc (2 mg/kg every other day) and wild-type mice were treated with i.p. injections of vehicle beginning at day 1 of life until day 28. On day 27, mice were injected with calcium NIR via tail vein. Aortas were harvested on day 28 and imaged with near-infrared fluorescence. Images are at the same magnification in all four panels with the scale bar indicating 3 mm. Wild-type mouse aortas did not exhibit calcium NIR signal while aortas from MGP$^{-/-}$ mice had a strong calcium NIR signal. Compared to vehicle-treated MGP$^{-/-}$ mice, the aortas of MGP$^{-/-}$ mice treated with either LDN or ALK3-Fc exhibited significantly reduced calcium NIR signals. This figure is taken from reference[25]. Please click here to view a larger version of this figure.

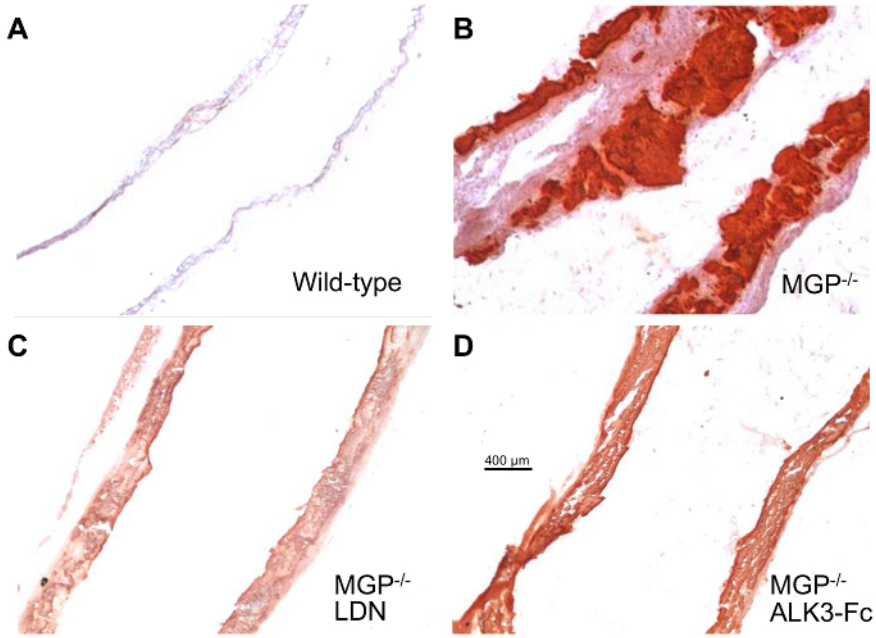

Figure 3: Pharmacologic Inhibition of BMP Signaling Prevents Aortic Calcification in MGP-deficient mice. Wild-type mice were treated with i.p. injections of vehicle (**A**) and $MGP^{-/-}$ mice were treated with either i.p. injections of vehicle (**B**), LDN (**C**, 2.5 mg/kg/day), or ALK3-Fc (**D**, 2 mg/kg every other day) beginning at day 1 of life until day 28. Aortas were harvested, sectioned, and stained for calcium with Alizarin red. Images were taken at the same magnification in all four panels with the scale bar indicating 400 µm. Similar to the calcium NIR signals in Figure 2, the Alizarin red staining demonstrates a heavy burden of calcification in the aortas of vehicle-treated $MGP^{-/-}$ mice. Calcification is decreased in the aortas of LDN- and ALK3-Fc-treated $MGP^{-/-}$ mice. This figure is taken from reference[25]. Please click here to view a larger version of this figure.

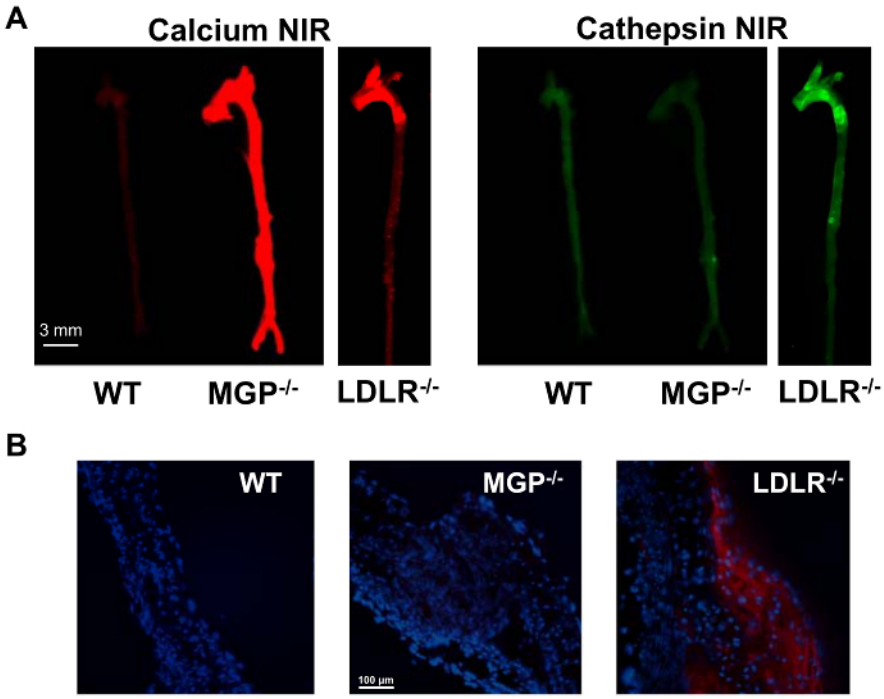

Figure 4: Simultaneous Determination of Aortic Calcification and Macrophage Infiltration with Calcium NIR and Cathepsin NIR. (**A**) Wild-type, MGP$^{-/-}$, and LDLR$^{-/-}$ mice fed a high-fat diet were injected with calcium NIR and cathepsin NIR via tail vein injection. Aortas were harvested 24 hr later and assessed with near-infrared fluorescence imaging. Images are at the same magnification with the scale bar indicating 3 mm. Wild-type mice exhibit virtually no aortic calcification or macrophage presence. The aortas from LDLR$^{-/-}$ mice have extensive calcification that co-localizes with macrophage accumulation. In contrast, MGP$^{-/-}$ mice have aortic calcification that occurs in the absence of macrophage infiltration. (**B**) Aortas were harvested from wild-type, MGP$^{-/-}$, and LDLR$^{-/-}$ mice fed a high-fat diet. These aortas were sectioned and stained for macrophages with an antibody specific for MAC-2. Nuclei were stained with DAPI. The lumenal surface is towards the right in each panel. Images were taken at the same magnification in all three panels with the scale bar indicating 100 µm. Similar to the findings in (**A**), there was no evidence of macrophage accumulation in the aortas of MGP$^{-/-}$ mice. This figure is a modified version of a figure from reference[25]. Please click here to view a larger version of this figure.

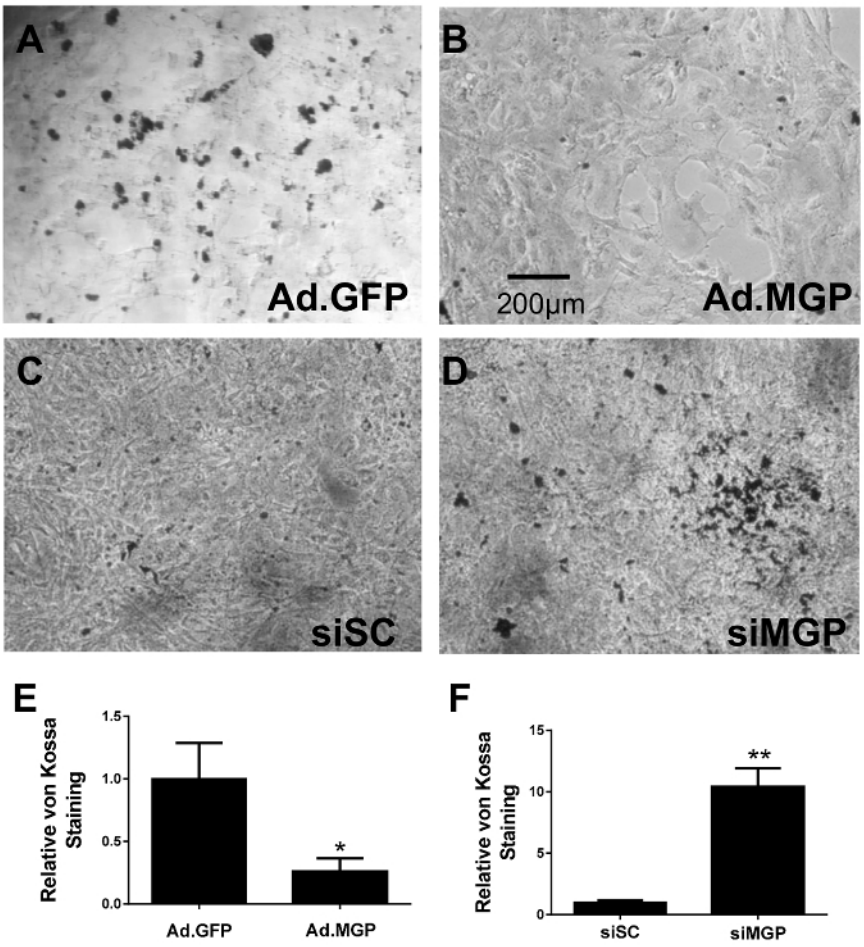

Figure 5: MGP Protects Cultured VSMCs from Calcification. Cultured aortic VSMCs were isolated from MGP$^{-/-}$ mice and infected with adenovirus expressing either GFP (**A**) or MGP (**B**). Aortic VSMCs isolated from wild-type mice were transfected with either control scrambled siRNA (**C**) or siRNA targeting MGP (**D**). Cells were grown in Calcification Media A for 7 days and subsequently fixed and stained with von Kossa. Images were taken at the same magnification in all four panels (**A**-**D**) with the scale bar indicating 200 μm. Serial fields of view were photographed and quantified for calcium staining using image J software after background subtraction (**E** and **F**), with error bars indicating SEM. This figure is a modified version of a figure from reference[25]. Please click here to view a larger version of this figure.

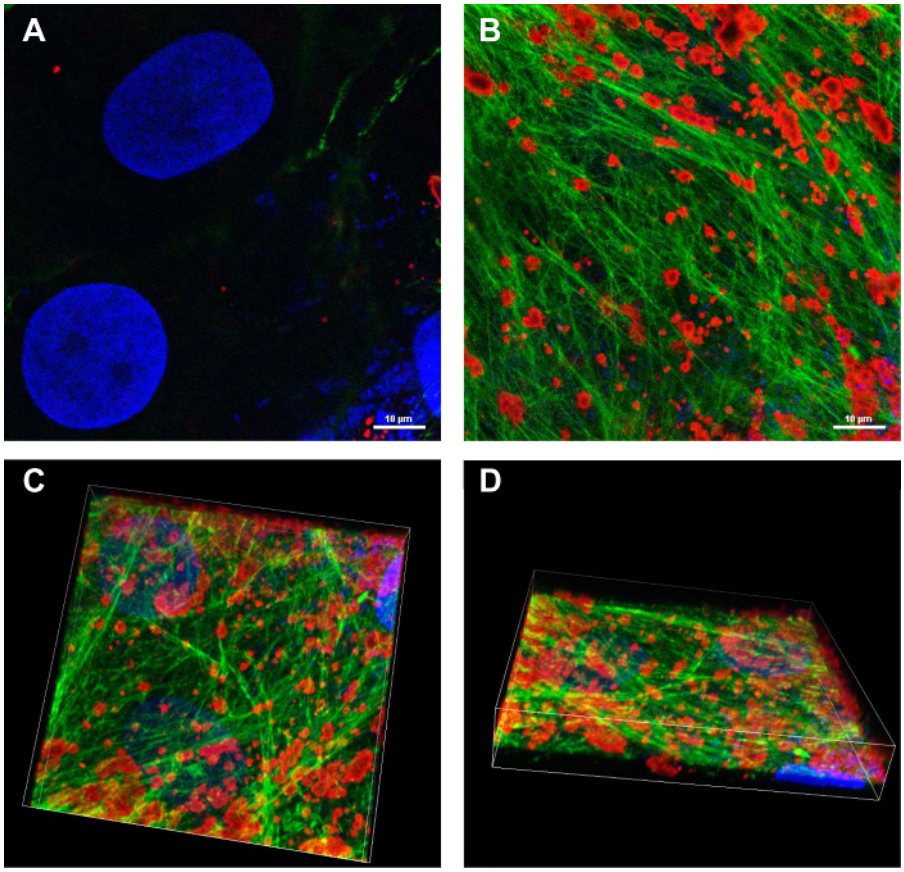

Figure 6: Calcium NIR Identifies Calcification in Association With the Extracellular Matrix *in vitro*. (**A**) Human coronary artery VSMCs cultured in Calcification Media B for 21 days were identified by nuclear staining using Hoechst dye. (**B**) An optical section obtained by confocal microscopy of calcium NIR staining (red) combined with a green-fluorescent collagen probe shows calcific mineral throughout the collagen matrix. Images **A**-**B** were taken at the same magnification with the scale bar indicating 10 µm. (**C** and **D**) Three-dimensional reconstructions show the entrapment of calcific mineral within the collagen matrix. Please click here to view a larger version of this figure.

Discussion

Arterial calcification is an important risk factor for cardiovascular disease in humans and may contribute directly to the pathogenesis of cardiovascular events.[1,5,52] Intimal calcium deposition in the thin fibrous caps of atherosclerotic disease has been proposed to increase local biomechanical stress and contribute to plaque rupture.[53,54] Medial calcification impacts clinical outcomes by increasing arterial stiffness, which can induce cardiac hypertrophy and affect cardiac function.[55] Therefore, understanding the molecular mechanisms that underlie vascular calcification will provide important insights into human disease and potentially identify novel targets for therapy.

Here, a method for detecting aortic calcification and macrophage accumulation in murine models of atherosclerosis and vascular calcification utilizing NIRF imaging is described.[9] It is critical to accurately inject the NIRF agents into the tail vein. This is a technique that requires significant practice before mastery is achieved.[56] Additionally, it is important to remove all of the peri-aortic fat from the aorta, as this fat can cause an autofluorescent signal at the same wavelength as the calcium NIR and cathepsin NIR signals. The use of NIRF agents has many important advantages over standard histologic methods of assessing vascular calcification and inflammation. In contrast to conventional histological techniques, these agents permit the quantification of whole aortic calcification and macrophage infiltration. Furthermore, they provide a more sensitive method for detecting early changes associated with the development of aortic calcification than histologic staining and can therefore offer mechanistic insights into earlier stages of disease.[9] Sites of early calcium NIR signal are associated with markers of bone formation including increased alkaline phosphatase activity as well as Runx2 and osteopontin gene expression. Moreover, the simultaneous use of spectrally distinct probes for calcification and cathepsin activity enables quantification and association of the spatiotemporal progression of both atheromatous and calcific disease.[9]

Identifying the spatial and temporal characteristics of vascular calcification and inflammation aids in our understanding of the underlying pathophysiologic mechanisms of vascular disease. For instance, the use of NIRF agents has demonstrated that in models of intimal calcification (ApoE$^{-/-}$ and LDLR$^{-/-}$ mice on a high-fat diet), vascular calcification co-localizes to sites of macrophage accumulation (**Figure 4**) and that calcification follows the accumulation of macrophages temporally.[9,11] Interestingly, no macrophage accumulation with cathepsin NIR was detected in the medial vascular calcification found in MGP-deficient mice.[25] Thus, from experiments utilizing NIRF agents, it can be concluded that although macrophage accumulation is associated with vascular intimal calcification, it is not required for vascular medial calcification.

Similar to its role in imaging and studying vascular disease, NIRF imaging has been utilized to study aortic valve disease.[47] Aortic valve disease is marked by lipid-laden macrophage and calcific lesions on the valve and exhibits similar underlying molecular mechanisms and genetic

determinants as atherosclerosis.[57-59] Aortic valve calcification causes impairment of leaflet function and is the primary cause of clinical aortic stenosis in the elderly. The only treatment currently available for symptomatic aortic stenosis is valve replacement. A better understanding of the molecular mechanisms of aortic valve disease is necessary to prevent the late-stage clinical complications of progressive aortic valve calcification. Utilization of NIRF agents as molecular imaging tools in animal models provides a sensitive method for assessing aortic valve disease at its earliest stages.[60]

Standard techniques to visualize coronary artery plaques have focused on the severity of stenosis, yet the majority of acute coronary syndromes result from rupture of non-flow-limiting plaques.[6] Biological processes within plaques, such as inflammation, serve as better predictors of plaque rupture than the degree of stenosis.[61] As opposed to conventional imaging techniques, NIRF imaging provides an opportunity to measure cellular activity (*i.e.*, macrophage proteolytic activity with a matrix metalloproteinase (MMP) activatable agent, proteolytic and elastolytic activity with cathepsin NIR, and osteogenic activity with calcium NIR).[9] This method therefore provides simultaneous functional and anatomical assessment of cardiovascular disease. NIRF imaging utilizes excitation wavelengths in the 650 to 900 nm range, which has the advantage of increased tissue penetration compared to light at a lower wavelength, thus allowing for greater depth assessment of disease lesions.[60] There is also reduced autofluorescent background signal of vascular tissue in the near-infrared wavelength range. Although this protocol focuses on the use of NIRF imaging *ex vivo*, NIRF imaging also represents a useful platform for longitudinal molecular imaging *in vivo*.[9] NIRF imaging, when combined with intravital microscopy, may have future diagnostic applications in humans.[61] However, a limitation of calcium NIR imaging longitudinally is that the bisphosphonate-derived probe may itself alter the physiologic process of calcification.[62]

Cardiovascular calcification is an actively regulated process that involves the transdifferentiation of VSMCs to an osteogenic phenotype.[25,41,42] To study the molecular mechanisms of VSMC-mediated calcification, a method for the isolation of primary murine aortic VSMCs for culture is provided. This method involves the initial enzymatic digestion of the aorta, followed by removal of the adventitial layer, and subsequent plating of smooth muscle cells. In this approach, it is critical to apply the digestion solution to the aorta for the appropriate amount of time. Too little time will not allow for an adequate separation of the adventitial layer from the medial layer, while too much time in the digestion solution will make the smooth, intact removal of the adventitial layer too challenging due to excess tissue destruction. In this protocol, 30 min is the recommended time for the aorta to be treated in digestion solution. This protocol is similar to that previously published[63] and has achieved adequate numbers of cells per murine aorta to perform *in vitro* studies (**Figure 5**). An alternative method for VSMC isolation does not involve enzymatic digestion but rather the direct culture of explanted aortic rings; this technique has been reported to yield fewer cells than the technique utilizing enzymatic digestion.[63,64]

Two different calcification media, either with βGP/Asc/DEX[65,66] or NaPhos,[25,43] are described that can be used to induce calcification of VSMCs. Both types of media have been used to calcify murine VSMCs with equivalent success. While the calcification media containing βGP/Asc/DEX has been used to calcify human VSMCs (**Figure 6**), the media containing NaPhos has not been effective in calcifying human VSMCs in our experience. Moreover, 21 - 28 days of culture of human VSMCs in Calcification Media B may be required before calcification is detected. Calcification of wild-type VSMCs *in vitro* was increased when expression levels of MGP were reduced with siRNA and calcification was reduced in $MGP^{-/-}$ VSMCs when MGP expression was restored (**Figure 5**). These findings are consistent with the aortic calcification observed in $MGP^{-/-}$ mice and suggest that this *in vitro* method of VSMC calcification serves as a useful model of *in vivo* calcification. It is important to note, however, that there are limitations in drawing conclusions regarding intact blood vessels from cultured VSMCs. Cultured VSMCs may lose their *in vivo* contractile properties, particularly at higher passages, in addition to developing changes in gene expression patterns, morphology, and rigidity.[67-70] VSMCs cultured in calcifying media do differentiate to an osteoblastic lineage before calcification, but do not exhibit a chondrocytic intermediate that is often observed *in vivo*.[71] It is therefore important that mechanistic conclusions drawn from cultured cells be validated in *in vivo* systems. One potential method of overcoming this limitation is to study VSMCs in their *in vivo* state using a cultured intact vessel ring.[70]

Two different methods are presented for detecting calcification of cultured VSMCs, the von Kossa method (**Figure 5**) and calcium NIR staining (**Figure 6**). Although used frequently to assess for calcification, the von Kossa method is somewhat limited by its reduced specificity for calcium crystals.[50] Calcium NIR is felt to be specific for calcification and is particularly advantageous in that it allows for simultaneous staining with additional spectrally-distinct fluorescent agents.[9] Future applications of this protocol utilizing calcium NIR with additional molecular probes may provide important insights into the mechanisms of calcification and may enable the rapid assessment of small molecule inhibitors of VSMC calcification in a high-throughput manner, to identify potential novel therapies for vascular calcification.

In summary, cardiovascular calcification is an important risk factor for and potential contributor to clinical disease. Knowledge of the mechanisms of cardiovascular calcification and atherosclerotic disease relies on both animal and cell-based models. Methodologies for assessing calcification in *in vivo*, *ex vivo*, and *in vitro* models are critical to advance our understanding of cardiovascular disease.

Disclosures

Massachusetts General Hospital has applied for patents related to small molecule inhibitors of BMP type I receptors and the application of ALK3-Fc to treat atherosclerosis and vascular calcification, and MD, PBY, KDB, and RM may be entitled to royalties.

Acknowledgements

This work was supported by the Sarnoff Cardiovascular Research Foundation (MFB and TET), the Howard Hughes Medical Institute (TM), the Ladue Memorial Fellowship Award from Harvard Medical School (DKR), the START-Program of the Faculty of Medicine at RWTH Aachen (MD), the German Research Foundation (DE 1685/1-1, MD), the National Eye Institute (R01EY022746, ESB), the Leducq Foundation (Multidisciplinary Program to Elucidate the Role of Bone Morphogenetic Protein Signaling in the Pathogenesis of Pulmonary and Systemic Vascular Diseases, PBY, KDB, and DBB), the National Institute of Arthritis and Musculoskeletal and Skin Diseases (R01AR057374, PBY), the National Institute of Diabetes and Digestive and Kidney Diseases (R01DK082971, KDB and DBB), the American Heart Association Fellow-to-Faculty Award #11FTF7290032 (RM), and the National Heart, Lung, and Blood Institute (R01HL114805 and R01HL109506, EA; K08HL111210, RM).

References

1. Go, A. S. *et al.* Heart disease and stroke statistics--2014 update: a report from the American Heart Association. *Circulation.* **129** (3), e28-e292 (2014).
2. Wilson, P. W. *et al.* Abdominal aortic calcific deposits are an important predictor of vascular morbidity and mortality. *Circulation.* **103** (11), 1529-1534 (2001).
3. Budoff, M. J. *et al.* Assessment of coronary artery disease by cardiac computed tomography: a scientific statement from the American Heart Association Committee on Cardiovascular Imaging and Intervention, Council on Cardiovascular Radiology and Intervention, and Committee on Cardiac Imaging, Council on Clinical Cardiology. *Circulation.* **114** (16), 1761-1791 (2006).
4. Greenland, P., LaBree, L., Azen, S. P., Doherty, T. M., & Detrano, R. C. Coronary artery calcium score combined with Framingham score for risk prediction in asymptomatic individuals. *Jama.* **291** (2) (2004).
5. Otsuka, F., Sakakura, K., Yahagi, K., Joner, M., & Virmani, R. Has our understanding of calcification in human coronary atherosclerosis progressed? *Arterioscler Thromb Vasc Biol.* **34** (4), 724-736 (2014).
6. Virmani, R., Burke, A. P., Farb, A., & Kolodgie, F. D. Pathology of the vulnerable plaque. *J Am Coll Cardiol.* **47** (8 Suppl), C13-18 (2006).
7. Amann, K. Media calcification and intima calcification are distinct entities in chronic kidney disease. *Clin J Am Soc Nephrol.* **3** (6), 1599-1605 (2008).
8. Aikawa, E. *et al.* Arterial and aortic valve calcification abolished by elastolytic cathepsin S deficiency in chronic renal disease. *Circulation.* **119** (13), 1785-1794 (2009).
9. Aikawa, E. *et al.* Osteogenesis associates with inflammation in early-stage atherosclerosis evaluated by molecular imaging in vivo. *Circulation.* **116** (24), 2841-2850 (2007).
10. Qiao, J. H. *et al.* Pathology of atheromatous lesions in inbred and genetically engineered mice. Genetic determination of arterial calcification. *Arterioscler Thromb.* **14** (9), 1480-1497 (1994).
11. Derwall, M. *et al.* Inhibition of bone morphogenetic protein signaling reduces vascular calcification and atherosclerosis. *Arterioscler Thromb Vasc Biol.* **32** (3), 613-622 (2012).
12. Luo, G. *et al.* Spontaneous calcification of arteries and cartilage in mice lacking matrix GLA protein. *Nature.* **386** (6620), 78-81 (1997).
13. Shobeiri, N., Adams, M. A., & Holden, R. M. Vascular calcification in animal models of CKD: A review. *Am J Nephrol.* **31** (6), 471-481 (2010).
14. Keutel, J., Jorgensen, G., & Gabriel, P. [A new autosomal-recessive hereditary syndrome. Multiple peripheral pulmonary stenosis, brachytelephalangia, inner-ear deafness, ossification or calcification of cartilages]. *Dtsch Med Wochenschr.* **96** (43), 1676-1681 (1971).
15. Munroe, P. B. *et al.* Mutations in the gene encoding the human matrix Gla protein cause Keutel syndrome. *Nat Genet.* **21** (1), 142-144 (1999).
16. Cormode, E. J., Dawson, M., & Lowry, R. B. Keutel syndrome: clinical report and literature review. *Am J Med Genet.* **24** (2), 289-294 (1986).
17. Fryns, J. P., van Fleteren, A., Mattelaer, P., & van den Berghe, H. Calcification of cartilages, brachytelephalangy and peripheral pulmonary stenosis. Confirmation of the Keutel syndrome. *Eur J Pediatr.* **142** (3), 201-203 (1984).
18. Ozdemir, N. *et al.* Tracheobronchial calcification associated with Keutel syndrome. *Turk J Pediatr.* **48** (4), 357-361 (2006).
19. Cranenburg, E. C. *et al.* Circulating matrix gamma-carboxyglutamate protein (MGP) species are refractory to vitamin K treatment in a new case of Keutel syndrome. *J Thromb Haemost.* **9** (6), 1225-1235 (2011).
20. Meier, M., Weng, L. P., Alexandrakis, E., Ruschoff, J., & Goeckenjan, G. Tracheobronchial stenosis in Keutel syndrome. *Eur Respir J.* **17** (3), 566-569 (2001).
21. Wang, Y. *et al.* Common genetic variants of MGP are associated with calcification on the arterial wall but not with calcification present in the atherosclerotic plaques. *Circ Cardiovasc Genet.* **6** (3), 271-278 (2013).
22. Cassidy-Bushrow, A. E. *et al.* Matrix gla protein gene polymorphism is associated with increased coronary artery calcification progression. *Arterioscler Thromb Vasc Biol.* **33** (3), 645-651 (2013).
23. Crosier, M. D. *et al.* Matrix Gla protein polymorphisms are associated with coronary artery calcification in men. *J Nutr Sci Vitaminol (Tokyo).* **55** (1), 59-65 (2009).
24. Liu, Y. P. *et al.* Inactive matrix Gla protein is causally related to adverse health outcomes: a Mendelian randomization study in a Flemish population. *Hypertension.* **65** (2), 463-470 (2015).
25. Malhotra, R. *et al.* Inhibition of bone morphogenetic protein signal transduction prevents the medial vascular calcification associated with matrix Gla protein deficiency. *PLoS One.* **10** (1), e0117098 (2015).
26. Demer, L. L., & Tintut, Y. Inflammatory, metabolic, and genetic mechanisms of vascular calcification. *Arterioscler Thromb Vasc Biol.* **34** (4), 715-723 (2014).
27. Rusanescu, G., Weissleder, R., & Aikawa, E. Notch signaling in cardiovascular disease and calcification. *Curr Cardiol Rev.* **4** (3), 148-156 (2008).
28. Leopold, J. A. Vascular calcification: Mechanisms of vascular smooth muscle cell calcification. *Trends Cardiovasc Med.* **25** (4), 267-274 (2015).
29. Bostrom, K. I., Rajamannan, N. M., & Towler, D. A. The regulation of valvular and vascular sclerosis by osteogenic morphogens. *Circ Res.* **109** (5), 564-577 (2011).
30. Hruska, K. A., Mathew, S., & Saab, G. Bone morphogenetic proteins in vascular calcification. *Circ Res.* **97** (2), 105-114 (2005).
31. Yao, Y. *et al.* Inhibition of bone morphogenetic proteins protects against atherosclerosis and vascular calcification. *Circ Res.* **107** (4), 485-494 (2010).
32. Bostrom, K. *et al.* Bone morphogenetic protein expression in human atherosclerotic lesions. *J Clin Invest.* **91** (4), 1800-1809 (1993).
33. Bragdon, B. *et al.* Bone morphogenetic proteins: a critical review. *Cell Signal.* **23** (4), 609-620 (2011).
34. Cai, J., Pardali, E., Sanchez-Duffhues, G., & ten Dijke, P. BMP signaling in vascular diseases. *FEBS Lett.* **586** (14), 1993-2002 (2012).
35. Lee, K. S. *et al.* Runx2 is a common target of transforming growth factor beta1 and bone morphogenetic protein 2, and cooperation between Runx2 and Smad5 induces osteoblast-specific gene expression in the pluripotent mesenchymal precursor cell line C2C12. *Mol Cell Biol.* **20** (23), 8783-8792 (2000).
36. Matsubara, T. *et al.* BMP2 regulates Osterix through Msx2 and Runx2 during osteoblast differentiation. *J Biol Chem.* **283** (43), 29119-29125 (2008).

37. Li, X., Yang, H. Y., & Giachelli, C. M. BMP-2 promotes phosphate uptake, phenotypic modulation, and calcification of human vascular smooth muscle cells. *Atherosclerosis.* **199** (2), 271-277 (2008).
38. Nakagawa, Y. *et al.* Paracrine osteogenic signals via bone morphogenetic protein-2 accelerate the atherosclerotic intimal calcification in vivo. *Arterioscler. Thromb. Vasc. Biol.* **30** (10), 1908-1915 (2010).
39. Cuny, G. D. *et al.* Structure-activity relationship study of bone morphogenetic protein (BMP) signaling inhibitors. *Bioorg Med Chem Lett.* **18** (15), 4388-4392 (2008).
40. Yu, P. B. *et al.* BMP type I receptor inhibition reduces heterotopic ossification. *Nat Med.* **14** (12), 1363-1369 (2008).
41. Schurgers, L. J., Uitto, J., & Reutelingsperger, C. P. Vitamin K-dependent carboxylation of matrix Gla-protein: a crucial switch to control ectopic mineralization. *Trends Mol Med.* **19** (4), 217-226 (2013).
42. Speer, M. Y. *et al.* Smooth muscle cells give rise to osteochondrogenic precursors and chondrocytes in calcifying arteries. *Circ Res.* **104** (6), 733-741 (2009).
43. Speer, M. Y., Li, X., Hiremath, P. G., & Giachelli, C. M. Runx2/Cbfa1, but not loss of myocardin, is required for smooth muscle cell lineage reprogramming toward osteochondrogenesis. *J Cell Biochem.* **110** (4), 935-947 (2010).
44. Steitz, S. A. *et al.* Smooth muscle cell phenotypic transition associated with calcification: upregulation of Cbfa1 and downregulation of smooth muscle lineage markers. *Circ Res.* **89** (12), 1147-1154 (2001).
45. Inoue, T., Plieth, D., Venkov, C. D., Xu, C., & Neilson, E. G. Antibodies against macrophages that overlap in specificity with fibroblasts. *Kidney Int.* **67** (6), 2488-2493 (2005).
46. Zaheer, A. *et al.* In vivo near-infrared fluorescence imaging of osteoblastic activity. *Nat Biotechnol.* **19** (12), 1148-1154 (2001).
47. Aikawa, E. *et al.* Multimodality molecular imaging identifies proteolytic and osteogenic activities in early aortic valve disease. *Circulation.* **115** (3), 377-386 (2007).
48. Lee, K. J., Czech, L., Waypa, G. B., & Farrow, K. N. Isolation of pulmonary artery smooth muscle cells from neonatal mice. *J Vis Exp.* (80), e50889 (2013).
49. Tang, Y., Herr, G., Johnson, W., Resnik, E., & Aho, J. Induction and analysis of epithelial to mesenchymal transition. *J Vis Exp.* (78) (2013).
50. Puchtler, H., & Meloan, S. N. Demonstration of phosphates in calcium deposits: a modification of von Kossa's reaction. *Histochemistry.* **56** (3-4), 177-185 (1978).
51. Krahn, K. N., Bouten, C. V., van Tuijl, S., van Zandvoort, M. A., & Merkx, M. Fluorescently labeled collagen binding proteins allow specific visualization of collagen in tissues and live cell culture. *Anal Biochem.* **350** (2), 177-185 (2006).
52. Johnson, R. C., Leopold, J. A., & Loscalzo, J. Vascular calcification: pathobiological mechanisms and clinical implications. *Circ Res.* **99** (10), 1044-1059 (2006).
53. Vengrenyuk, Y. *et al.* A hypothesis for vulnerable plaque rupture due to stress-induced debonding around cellular microcalcifications in thin fibrous caps. *Proc Natl Acad Sci U S A.* **103** (40), 14678-14683 (2006).
54. Maldonado, N. *et al.* A mechanistic analysis of the role of microcalcifications in atherosclerotic plaque stability: potential implications for plaque rupture. *Am J Physiol Heart Circ Physiol.* **303** (5), H619-628 (2012).
55. Toussaint, N. D., & Kerr, P. G. Vascular calcification and arterial stiffness in chronic kidney disease: implications and management. *Nephrology (Carlton).* **12** (5), 500-509 (2007).
56. Vines, D. C., Green, D. E., Kudo, G., & Keller, H. Evaluation of mouse tail-vein injections both qualitatively and quantitatively on small-animal PET tail scans. *J Nucl Med Technol.* **39** (4), 264-270 (2011).
57. Smith, J. G. *et al.* Association of low-density lipoprotein cholesterol-related genetic variants with aortic valve calcium and incident aortic stenosis. *Jama.* **312** (17) (2014).
58. Thanassoulis, G. *et al.* Genetic associations with valvular calcification and aortic stenosis. *N Engl J Med.* **368** (6), 503-512 (2013).
59. Otto, C. M., Kuusisto, J., Reichenbach, D. D., Gown, A. M., & O'Brien, K. D. Characterization of the early lesion of 'degenerative' valvular aortic stenosis. Histological and immunohistochemical studies. *Circulation.* **90** (2), 844-853 (1994).
60. New, S. E., & Aikawa, E. Molecular imaging insights into early inflammatory stages of arterial and aortic valve calcification. *Circ Res.* **108** (11), 1381-1391 (2011).
61. Jaffer, F. A., Libby, P., & Weissleder, R. Optical and multimodality molecular imaging: insights into atherosclerosis. *Arterioscler Thromb Vasc Biol.* **29** (7), 1017-1024 (2009).
62. Stern, P. H. Antiresorptive agents and osteoclast apoptosis. *J Cell Biochem.* **101** (5), 1087-1096 (2007).
63. Ray, J. L., Leach, R., Herbert, J. M., & Benson, M. Isolation of vascular smooth muscle cells from a single murine aorta. *Methods Cell Sci.* **23** (4), 185-188 (2001).
64. Chamley-Campbell, J., Campbell, G. R., & Ross, R. The smooth muscle cell in culture. *Physiol Rev.* **59** (1), 1-61 (1979).
65. Trion, A., Schutte-Bart, C., Bax, W. H., Jukema, J. W., & van der Laarse, A. Modulation of calcification of vascular smooth muscle cells in culture by calcium antagonists, statins, and their combination. *Mol Cell Biochem.* **308** (1-2), 25-33 (2008).
66. Mori, K., Shioi, A., Jono, S., Nishizawa, Y., & Morii, H. Dexamethasone enhances In vitro vascular calcification by promoting osteoblastic differentiation of vascular smooth muscle cells. *Arterioscler Thromb Vasc Biol.* **19** (9), 2112-2118 (1999).
67. Thyberg, J. Differentiated properties and proliferation of arterial smooth muscle cells in culture. *Int Rev Cytol.* **169** 183-265 (1996).
68. Dinardo, C. L. *et al.* Vascular smooth muscle cells exhibit a progressive loss of rigidity with serial culture passaging. *Biorheology.* **49** (5-6), 365-373 (2012).
69. Metz, R. P., Patterson, J. L., & Wilson, E. Vascular smooth muscle cells: isolation, culture, and characterization. *Methods Mol Biol.* **843** 169-176 (2012).
70. Proudfoot, D., & Shanahan, C. Human vascular smooth muscle cell culture. *Methods Mol Biol.* **806** 251-263 (2012).
71. Hruska, K. A. Vascular smooth muscle cells in the pathogenesis of vascular calcification. *Circ Res.* **104** (6), 710-711 (2009).

